AIChE Journal, Volume 65, Issue 4, April 2019, pp. 1256-1268
DOI:10.1002/aic.16531

The combined effect of H_2O and SO_2 on the simultaneous calcination/sulfation reaction in CFBs

Liang Chen[1], Chunbo Wang [1], Fan Zhao[1], Chan Zou[1], Edward J. Anthony[2*]
[1]School of Energy and Power Engineering, North China Electric Power University, Baoding 071000, China
[2]Institute for Energy and Resource Technology, School of Energy, Environment and Agrifood, Cranfield University, Cranfield, Bedfordshire MK43 0AL, UK
[*]Corresponding author. E-mail address: b.j.anthony@cranfield.ac.uk

Abstract

The combined effect of H_2O and SO_2 on the reaction kinetics and pore structure of limestone during simultaneous calcination/sulfation reactions under circulating fluidized bed (CFB) conditions was first studied in a constant-temperature reactor. H_2O can accelerate the sulfation reaction rate in the slow-sulfation stage significantly but has a smaller effect in the fast-sulfation stage. H_2O can also accelerate the calcination of $CaCO_3$, and should be considered as a catalyst, since the activation energy for the calcination reaction was lower in the presence of H_2O. When the limestone particles are calcining, SO_2 in the flue gas can react with CaO on the outer particle layer and the resulting $CaSO_4$ blocks the CaO pores, increases the diffusion resistance of CO_2 and, in consequence, decreases the calcination rate of $CaCO_3$. Here, gases containing 15% H_2O and 0.3% SO_2 are shown to increase the calcination rate. This means that the accelerating effect of 15% H_2O on $CaCO_3$ decomposition is stronger than the impeding effect caused by 0.3% SO_2. The calcination rate of limestone particles was controlled by both the intrinsic reaction and the CO_2 diffusion rate in the pores, but the intrinsic reaction rate played a major role as indicated by the effectiveness factors determined in this work. This may explain the synergic effect of

Published by Wiley. This is the Author Accepted Manuscript issued with: Creative Commons Attribution Non-Commercial License (CC:BY:NC 4.0).
The final published version (version of record) is available online at DOI:10.1002/aic.16531. Please refer to any applicable publisher terms of use.

H_2O and SO_2 on $CaCO_3$ decomposition observed here. Finally, the effect of H_2O and SO_2 on sulfur capture in a 600 MWe CFB boiler burning petroleum coke is also analyzed. The sulfation performance of limestone evaluated by simultaneous calcination/sulfation is shown to be much higher than that by sulfation of CaO. Based on our calculations, a novel use of the wet flue gas recycle method was put forward to improve the sulfur capture performance for high-sulfur, low-moisture fuels such as petroleum coke.

Key words: Calcination; Sulfation; Simultaneous reaction; Limestone; Kinetics; H_2O

Introduction

With the industrial application of 600 MWe supercritical circulating fluidized bed (CFB) boilers and the advanced development of 1000 MWe CFBs, these boilers will be widely used for power generation, especially when combusting poor-quality fuels like low-rank coals, petroleum coke and refuse-derived fuels.

In-situ desulfurization is one of the greatest advantages of CFB boilers. However, the low sulfur capture efficiency and low calcium utilization represent their greatest deficiencies. Economical but effective techniques to improve the sulfur capture performance in CFB boilers are still being sought. But this requires a comprehensive understanding of the sulfur capture process.

Limestone is the normal sorbent for desulfurization in CFBs. To capture SO_2, limestone will experience the calcination reaction (1) and sulfation reaction (2) in the furnace.

$$CaCO_3 \rightarrow CaO + CO_2 \quad (1)$$

$$CaO + SO_2 + 1/2O_2 \rightarrow CaSO_4 \quad (2)$$

Over the past several decades, many researchers have explored these reactions [1-4]. The calcination of limestone is reversible, and the reaction rate is usually related to three steps [5]: heat transfer; CO_2 diffusion; and the intrinsic reaction. Which of these steps has a greater impact on the calcination rate depends on factors like temperature, CO_2 concentration, particle size, etc. Generally, a higher temperature, low CO_2 concentration and smaller particle size will increase the calcination rate of limestone [5-7].

The sulfation reaction of CaO may also be controlled by heat transfer, SO_2 diffusion in the pores of CaO, solid state diffusion through the $CaSO_4$ product layer or the intrinsic sulfation reaction rate. To increase the sulfation rate, a smaller particle size, higher SO_2 concentration and optimum temperature are suggested [8-10]. Limestone particles in a CFB are recirculated and sulfated for periods of hours, and the long-term sulfation reaction can usually be divided into a fast-reaction stage and a slow-reaction stage [11]. The common consensus is that the fast-sulfation stage is controlled by the intrinsic reaction rate or SO_2 diffusion, while in the slow stage the diffusion through the $CaSO_4$ product layer is the major resistance to sulfation [12].

H_2O is one of the main components in the gas produced from coal firing, and usually accounts for 10-20% of CFB flue gases. Investigation has shown that the calcination of $CaCO_3$, sintering and sulfation of CaO are all significantly affected by H_2O [13, 14]. Many investigations have reported that the calcination of $CaCO_3$ can be

greatly accelerated by H_2O [11, 15], even at very low steam pressures [14]. Researchers have put forward different theories to explain the effect of H_2O on $CaCO_3$ decomposition. Burnham et al. [16] suggested that H_2O can lower the decomposition temperature of $CaCO_3$, while the research of Wang et al. [14] suggested that H_2O may weaken the bonding between C-O in $CaCO_3$.

H_2O can also affect the sulfation of CaO [11]. Some investigations [17, 18] have reported that H_2O had little influence on the sulfation reaction in the fast stage, but significantly accelerated the reaction rate in the slow-sulfation stage. Based on this phenomenon, some researchers speculated that H_2O may accelerate solid-state ion diffusion in the $CaSO_4$ product layer [19, 20], but the mechanism is as yet unclear.

As discussed above, the calcination and sulfation reactions of limestone have been thoroughly studied, but most of the studies are conducted as follows: calcine limestone particles in air or N_2 atmosphere;; then test the sulfation performance of the resulting CaO. In other words, most previous studies have considered the calcination reaction and the sulfation reaction as separate processes ("calcination-then-sulfation" reactions). However, this does not represent what is actually occurring in CFBs. The actual process proceeds as follows: after limestone reaches hot flue gases containing SO_2, the calcination and sulfation reactions occur simultaneously, and the two reactions affect each other. We call this process the 'simultaneous calcination/sulfation of limestone' and have carried out preliminary investigations on it [21-23]. Some important phenomena were demonstrated in our earlier work, in particular, the decomposition rate of limestone particles was impeded by SO_2, and

some of the $CaCO_3$ did not decompose completely even after 90-min reaction in the presence of 0.38% SO_2. Hence, the simultaneous calcination/sulfation reaction, rather than the calcination of $CaCO_3$ and the sulfation of CaO, more accurately describes what is happening to limestone in a CFB. Unfortunately, this has not been taken into account in the bulk of research done to date.

In a CFB, it takes several hundred seconds for the limestone particles to decompose completely, and during this process $CaSO_4$ forms in their pores. Since the calcination usually occurs from the particle surface inward, the pores in the outer CaO layer serve as the diffusion path for CO_2. If a pore is filled by $CaSO_4$, the diffusion resistance of CO_2 increases and, consequently, the calcination rate of the particle will be retarded. If all the pores are blocked before complete decomposition occurs, some $CaCO_3$ will be sealed in the inner particle and remain undecomposed during the entire sulfation process. Where this is the case, much of the pre-existing research on $CaCO_3$ calcination and CaO sulfation fails to describe the actual reaction characteristics of limestone in a CFB.

As is well known, one of the main problems for SO_2 capture in CFBs is that the utilization of limestone is much lower than the theoretical value. Although there have been decades of investigation, this problem is still unresolved [1]. Moreover, there are still many unclarified questions on the sulfation of limestone in CFBs [24]. To know more about the real reaction characteristics, the interaction of the two reactions in the simultaneous calcination/sulfation process requires attention. It is worth noting that the issue of reaction product interfering with limestone calcination is not only limited

to SO_2 capture in CFBs, but is also important for other processes like CO_2 capture by calcium looping [25-27]. Therefore, in our previous work [21, 22], the characteristics of the simultaneous calcination/sulfation reaction were investigated by thermogravimetric analysis (TGA).

However, some knowledge gaps still remained. First, how does SO_2 affect the pore structure of CaO during the simultaneous reactions? Second, how does H_2O influence the calcination and sulfation kinetics as well as the pore structure of sorbents? Third, what is the combined effect of H_2O and SO_2 on the reactions and pore evolution of sorbents?

The most probable reason for these questions not being answered is that it is impossible to measure the calcination and sulfation rates separately in a normal commercial TGA. Moreover, the sample collected from one test in a commercial TGA is very small (about 10 mg), so it needs about 100 repetitions to collect enough samples (about 1 g) for the pore structure measurement. To answer these questions while addressing the shortcomings of TGA, a specially designed experimental system was employed here. With this equipment it is feasible to measure the calcination and sulfation rates separately [23]. The sample collected from one test in this system is about 50 mg, so it is easier to obtain enough sample for the pore structure measurement.

To fill the knowledge gaps on simultaneous calcination/sulfation of limestone in CFBs, the combined effect of SO_2 and H_2O on reaction kinetics and the pore structure of sorbents was studied for the first time. The SO_2 emission in a 600 MWe CFB burning petroleum coke was calculated to show how SO_2 and H_2O affect the in-situ

sulfur capture performance. Based on these calculations, the novel use of the wet flue gas recycle method was recommended to optimize the SO_2 capture in air-fired CFB.

Experiments and Calculations

Experimental system and procedure

Baoding and Xinxiang limestone were used for the tests. The limestone was milled and sieved to a narrow particle size range (0.4-0.45 mm). Their chemical components are listed in Table 1 according to X-ray fluorescence (XRF) elemental analysis.

The pore structures of the two limestones after being calcined completely under the same conditions (850 ºC, 15% CO_2 and 85% N_2) were measured by the N_2 adsorption analyzer (Micromeritics TriStar Ⅱ 3020), and results are summarized in Table 2.

The experimental system is shown in Fig. 1. The main reactor is a horizontal tube furnace (40 mm internal diameter, 800 mm length, accuracy of 2 °C). Synthetic flue gas was composed of mixed gases of CO_2, SO_2, O_2, N_2 and H_2O. The flux of each gas was controlled by flowmeters, except for H_2O. The H_2O vapor was generated from the evaporation of water injected into a heated tube (200 °C), and its flow was controlled by an injection pump. A total gas flux of 1.2 dm^3/min was used after ascertaining that this flux was high enough to eliminate external gas diffusion resistance. After the furnace reached the set temperature and was purged by synthetic flue gas for 15 min, the sample (80 ± 2 mg) was loaded into a quartz boat, and its mass was continually measured by a mass monitor (accuracy 0.1 mg) and recorded by computer. Our previous work [11, 23, 28] with this system showed it has sufficient

accuracy for this type of study.

When limestone is calcined and sulfated simultaneously, the calcination ratio cannot be calculated directly from the mass data. To determine the calcination ratio, the sample at a given reaction time was removed quickly from the furnace and cooled in N_2. Then the sample was weighed, crushed and calcined again in pure N_2, until the sample was calcined totally. The calcination ratio of the sample was calculated by:

$$X_c = 1 - \frac{m_t x_t}{\lambda m_0} \tag{3}$$

where x_t is the mass fraction of the undecomposed $CaCO_3$ in the sample, $x_t = (1 - m_2/m_1)\left(M_{CaCO_3}/M_{CO_2}\right)$; m_0 is the initial sample mass; m_t is the sample mass after a given reaction duration; m_1 is the mass of sample after crushing; m_2 is the mass of the sample after being totally calcined; λ is the $CaCO_3$ mass fraction of limestone, assuming that other impurities don't react; and M_{CaCO_3} and M_{CO_2} are the mole mass of $CaCO_3$ and CO_2, respectively.

The sulfation ratio of the limestone samples can be calculated by the expression:

$$X_S = \frac{\frac{m_t}{\lambda m_0} + (1 - \frac{m_t x_t}{\lambda m_0})\frac{M_{CO_2}}{M_{CaCO_3}} - \frac{1}{\lambda}}{\left(M_{CaSO_4} - M_{CaO}\right)/M_{CaCO_3}} \tag{4}$$

where M_{CaO} and M_{CaSO_4} are the molecular mass of CaO and $CaSO_4$, respectively.

Since the calcination ratio curve was not smooth, the calcination rate cannot be obtained by the derivative of the X_c–time curves. So, an average calcination rate $\overline{r}_c$ before a given reaction time t was used to describe the calcination speed. The $\overline{r}_c$ value was calculated by:

$$\overline{r}_c = X_{c,t}/t \tag{5}$$

where $X_{c,t}$ is the calcination ratio at time t.

All the tests were carried out in triplicate (or more) to assure repeatability, and in all tests the standard deviations of the calcination ratio were less than 1%. All the sample mass curves in the figures were normalized to initial sample mass of one unit (the normalized mass equals the sample mass divided by its initial mass). The pore structures of the calcined samples were measured by the N_2 adsorption method. Table 3 summarizes the experimental conditions.

Calculations

To demonstrate the effect of H_2O and SO_2 content on sulfur capture, a simplified model based on energy and material balances was established to calculate the limestone consumption, desulfurization efficiency and the SO_2 emission in an industrial CFB boiler. The fuel consumption W_{fuel} (t/h) for a CFB boiler can be calculated by

$$W_{\text{fuel}} = \frac{P \cdot C_{\text{sc}} \cdot Q_{\text{sc}}}{Q_{\text{ar}}} \tag{6}$$

where P is the electric power of the boiler, MWe; C_{sc} is the standard coal consumption for power generation, kg/kWh; Q_{sc} is the calorific value of the standard coal, 29310 kJ/kg; and Q_{ar} is the net calorific value of the fuel as received, kJ/kg.

The total in-situ desulfurization efficiency is

$$\alpha_{\text{s}} = Ca/S \cdot X_{\text{s}} + \alpha_{\text{s,self}} \tag{7}$$

in which Ca/S is the calcium/sulfur molar ratio, $\alpha_{s,\text{self}}$ is the self-desulfurization efficiency of fuels, and X_{S} is the utilization of calcium.

To reach a given desulfurization efficiency of α_{s}, the limestone consumption W_{ls} (t/h, ignoring impurities) can be calculated by

$$W_{ls} = W_{fuel} S_{ar} \left(\alpha_s - \alpha_{self} \right) M_{CaCO_3} / \left(X_s M_s \right) \quad (8)$$

in which S_{ar} is the sulfur content of the fuel, kg/kg; M_{CaCO_3} =100 g/mol; and M_s =32 g/mol.

The SO_2 emission S_{em} (t/h) after the desulfurization process is

$$S_{em} = 2 W_{fuel} S_{ar} \left(1 - \alpha_s \right) \quad (9)$$

Results and Discussion

Effect of H_2O on kinetics of simultaneous calcination/sulfation reaction

The influence of H_2O on the simultaneous calcination/sulfation reaction was tested first. All tests were done at 850°C, under 15% CO_2 + 0.3% SO_2 + 3% O_2, with 0% or 15% H_2O, and N_2 balance. For comparison, the effect of H_2O on the calcination-then-sulfation of limestone was also tested, as shown in Fig. 2.

Fig. 2 shows that the mass of all samples declined first and then rose, and there was a minimum mass point for each curve. For convenience, the curves in Fig. 2 were divided into two stages by the minimum mass point, designated as the mass-loss stage and the mass-growth stage, respectively. The mass-loss stage was dominated by the calcination reaction, and the mass-growth stage by the sulfation reaction. But it should be noted that in the simultaneous calcination/sulfation reaction, the minimum mass point occurs when the mass loss rate caused by the calcination reaction equals the mass gain rate caused by the sulfation reaction, not the end of the calcination reaction or the beginning of the sulfation reaction like that in the calcination-then-sulfation reaction. This means that both calcination and sulfation reactions occur in both stages

in the simultaneous calcination/sulfation reaction [21]. The mass-growth stage can also be divided into two stages according to the sulfation rate, namely the fast-sulfation stage (from the minimum mass point to 40 min) and the slow-sulfation stage (beyond 40 min).

The mass-loss stage is discussed below. First, examining the mass-growth stage, it is found that the samples in the simultaneous calcination/sulfation reaction had higher mass, which implies a higher sulfation ratio than that of the calcination-then-sulfation reaction. The final samples, after being crushed and re-calcined, did not lose further mass. This means that there was no undecomposed $CaCO_3$ in the final samples, so their sulfation ratio can be calculated based on formula (4) with $x_t = 0$. Taking conditions without H_2O for example, the final sulfation ratio of the simultaneous calcination/sulfation reaction was 0.22, which was 25.5% higher than that (0.175) in the calcination-then-sulfation reaction.

Fig. 2 shows that H_2O significantly accelerated the sulfation rate in the slow-sulfation stage but had less influence in the fast-sulfation stage as compared with conditions without H_2O. Taking the simultaneous calcination/sulfation reaction for example, the sulfation ratio of samples in 15% H_2O is 0.288, which is much higher than that (0.22) in 0% H_2O. A preliminary explanation for the effect of H_2O on the sulfation reaction supports the idea that H_2O accelerates the sulfation rate in the slow sulfation stage by improving the solid-state ion diffusion in the $CaSO_4$ product layer [17, 19]. But why H_2O can act in this way needs more investigation. Wang et al. [22] found that the unreacted CaO cores covered by $CaSO_4$ in the presence of H_2O were smaller

and more dispersed, which may increase the reaction surface and accelerate the sulfation rate.

Regarding the mass-loss stage, Fig. 3(a) shows greater detail for that stage from Fig. 2. The calcination ratios were calculated as in Fig. 3(b).

First, considering the influence of H_2O on the calcination reaction, Fig. 3(a) shows that H_2O accelerated the mass loss rate of calcination significantly, both in the presence and absence of SO_2. H_2O also accelerated the calcination rate, as shown in Fig. 3(b). Taking conditions without SO_2 for example, the average calcination rate (7.34×10^{-3} /s) before 120 s with 15% H_2O is 28.3% higher than that (5.72×10^{-3}/s) without H_2O. The mechanism of the H_2O effect on calcination is discussed below.

Second, considering the effect of SO_2 on the calcination rate by looking at the two curves obtained without H_2O, the mass loss rate of the sample without SO_2 was faster than that in the presence of 0.3% SO_2. In addition, the final mass of the sample was different. The lowest mass (0.594) of the sample calcined with 0.3% SO_2 was about 4.0% higher than that (0.571) of the sample calcined without SO_2. From Fig. 3(b), the average calcination rate before 120 s in 0.3% SO_2 (5.06×10^{-3}/s) was 13.0% lower than that (5.72×10^{-3}/s) without SO_2, which means that the calcination rate was slowed by the presence of 0.3% SO_2. A similar effect of SO_2 was found under conditions with 15% H_2O.

Interestingly, when both H_2O and SO_2 were present, Fig. 3(b) shows that the calcination rate under 15% H_2O with 0.3% SO_2 is slower than that under 15% H_2O and no SO_2, but faster than that without SO_2 and H_2O. This means that, on the one

hand, the accelerating effect of H_2O and the impeding effect of SO_2 can coexist when they change the calcination rate; and on the other hand, the accelerating effect of 15% H_2O is more significant than the impeding effect of 0.3% SO_2.

One more phenomenon to be noted in Fig. 3(b) is that the samples under all four conditions were calcined completely at 300 s. This is different from the findings on Massicci limestone in the work of Wang et al. [21], where they found that the samples which experienced 90 min of reaction still contained 3-5% mass fraction of undecomposed $CaCO_3$. The reason may be that the sulfation reactivity of the limestone used in the present work is lower than for Massicci limestone, as has been pointed out elsewhere [23].

To demonstrate that the accelerating effect of H_2O in Fig. 3 is not limited to only 15% H_2O, another H_2O concentration (8%) was tested and compared with that of 0% and 15% H_2O. Limestone with 0.4-0.45 mm particle size was used, and SO_2 was 0.3% as before (see Fig. 4).

From Fig. 4(a), it can be seen that with H_2O increasing from 0 to 8% and further to 15%, the mass loss rate of the sample continued to increase. From Fig. 4(b), with H_2O increasing from 0% to 8% and 15%, the average calcination rate before 120 s increased from 5.06×10^{-3}/s to 5.92×10^{-3}/s and further to 6.40×10^{-3}/s. So, the calcination rate increased with the increasing H_2O concentration in the range 0-15%.

Since SO_2 concentration has significant influence on the sulfation rate, the calcination performance of limestone can be expected to be different under different SO_2 concentrations. To further study the effect of SO_2 concentration on the calcination,

calcinations were done under 0/0.15/0.3% SO_2 with 15% H_2O (see results in Fig. 5).

From Fig. 5(a), the mass loss rate under 0.15% SO_2 was lower than that without SO_2. When the SO_2 concentration was raised to 0.3%, the mass loss rate decreased further. And from Fig. 5(b), it can be seen that the calcination rate can also be influenced by the SO_2 concentration. Taking the average calcination rate before 120 s for example, when SO_2 concentration increased from 0 to 0.15% and 0.3%, the calcination rate decreased from 7.34×10^{-3}/s to 6.84×10^{-3}/s and further to 6.40×10^{-3}/s. So, in the range tested, a higher concentration of SO_2 will decrease the calcination rate more significantly.

SO_2 may react with CaO in the calcination stage, and fill or block the pores in the CaO layer. With higher SO_2 concentration in the atmosphere, the sulfation rate will be higher and more $CaSO_4$ will form in the pores. With more pores filled, the CO_2 diffusion resistance is higher and, in consequence, the calcination is slower.

To demonstrate that the combined effect of H_2O and SO_2 was not limited to one limestone, another limestone, Xinxiang limestone was also tested. The test conditions were the same as in Fig. 3, and the results are shown in Fig. 6.

The reaction curves of Xinxiang limestone shown in Fig. 6 are similar to those of Baoding limestone in Fig. 3. The calcination rate was accelerated significantly with 15% H_2O, with or without 0.3% SO_2; while 0.3% SO_2 decreased the calcination reaction also. As shown in Table 2, the pore surface area, pore volume and width of the two limestones used in this work were very different from each other. The pore surface area of Baoding limestone is much larger than that of the Xinxiang limestone,

but the average pore width of Baoding limestone is much narrower, which means that they are two distinct types of limestone. Despite their different pore structures, the combined effect of H_2O and SO_2 in Fig. 6 was also similar to that reported in Fig. 3. So, the effect of H_2O and SO_2 on calcination are clearly not limited to a particular limestone.

Mechanisms

As discussed above, H_2O can accelerate the calcination rate of limestone, and SO_2, on the contrary, slows down the calcination reaction. When both H_2O and SO_2 were present, the acceleration caused by 15% H_2O is stronger than the reduction in rate by 0.3% SO_2 in this work and, hence, the calcination rate increases (Fig. 3). The mechanisms for how H_2O and SO_2 separately affect the calcination were also studied first, then the mechanism for their combined effect was investigated.

Mechanism of the effect of H_2O on limestone calcination

The effect of H_2O on calcination has been investigated by many researchers, and one speculation is that H_2O catalyzes the decomposition of $CaCO_3$ [14, 15, 29]. A direct method of proving the catalytic effect is to measure the change in the activation energy. However, little information was available on this in the literature. Using a fluidized bed reactor, Wang et al. [29] found that the activation energy for calcination with 15% H_2O is lower than that without H_2O. Wang et al. [14] reported that H_2O may accelerate the decomposition of $CaCO_3$ by weakening the bonding between CaO and CO_2, but the activation energies they obtained (247 kJ/mol for 21.35% H_2O and 197 kJ/mol without H_2O) are contradictory to the observed phenomenon that H_2O

accelerated the calcination rate.

Here in this work, the apparent activation energies for the calcination of limestone with or without H_2O were measured and compared. The calcinations were tested under four temperatures (820, 850, 880 and 910 °C), with 0 and 15% H_2O (no SO_2) in the system of Fig. 1. The calcination reaction rate constant k_c is calculated by:

$$r_c = k_c\left(1 - C_{CO_2}\big/C^e_{CO_2}\right) \tag{10}$$

in which r_c is the calcination rate, calculated by formula (5) before the time corresponding to $X_{c,t}$=0.4; C_{CO_2} is the concentration of CO_2 at the calcination point, equal to that in the reaction atmosphere based on the kinetic controlling mechanism in the early calcination stage. $C^e_{CO_2}$ is the equilibrium CO_2 concentration at the reaction temperature, which can be calculated by the formula of Baker [30]. Generally, k_c is in the form of the Arrhenius equation (in linear expression):

$$\ln k_c = -E_a/(RT) + \ln k_0 \tag{11}$$

Hence, the activation energy (E_a) can be calculated with k_c at different temperatures (T). In Fig. 7, the k_c values under the four temperatures were fitted by equation (11) with least squares. The fitting equations as well as E_a and k_0 are calculated in Table 4.

From Table 4, the activation energy for calcination without H_2O and with 15% H_2O were 148.4 kJ/mol and 129.6 kJ/mol, respectively. The activation energies are very similar to the values reported by Wang et al. [29]. The activation energy of calcination with 15% H_2O is about 13.6% lower than that without H_2O. The decrease in the activation energy indicated that H_2O catalyzed the calcination of $CaCO_3$. As noted by Wang et al. [14], H_2O had a stronger binding ability to the active sites $CaCO_3$* than CO_2,

and the adsorption of H_2O on the active sites may weaken the bonding between CO_2 and CaO and increase the decomposition rate.

For reversible reactions, the catalyst can accelerate both the forward and backward reaction. If H_2O can catalyze the calcination of $CaCO_3$, it should also accelerate the carbonation of CaO. Interestingly, the acceleration of CaO carbonation by H_2O has been reported by many other researchers [31, 32]. Wang et al. [33] found that H_2O can also decrease the activation energy of the CaO carbonation reaction. In conclusion, the accelerating effect of H_2O on the calcination of $CaCO_3$ is quite likely to be catalysis.

Mechanism of the effect of SO_2 on limestone calcination

As discussed above, the sulfation reaction will occur when limestone particles are calcined in an atmosphere containing SO_2 and impede the calcination rate. The impeding effect of SO_2 on the calcination is speculated to occur by $CaSO_4$ filling or blocking the pores of CaO. To prove this hypothesis, the pore structure of particles was measured by the N_2 adsorption method, and the closed-pore volume blocked by the formed $CaSO_4$ under 0.3% SO_2 was calculated. Then the effect of $CaSO_4$ on the diffusion resistance of CO_2 was calculated and analyzed.

The Baoding limestone particles calcined for a given time were collected. The pore surface area and pore volume of samples calcined with or without 0.3% SO_2 are compared in Fig. 8. The test was at 850 °C, without H_2O.

As shown in Fig. 8, both the pore surface area and pore volume increased with calcination time under each condition. What should be noted is that the minimum mass point for calcination with 0.3% SO_2 was reached at about 275 s, and the

calcination was complete at 300 s as described in Fig. 3. Hence, the increase of the pore volume will not continue after 300 s, and only samples before 300 s were measured here. Compared with the samples without SO_2, both the pore surface area and pore volume under 0.3% SO_2 decreased significantly. In addition, the difference between the curves increased with reaction time, which means that with the calcination going on, more pores of CaO were filled or closed by the produced $CaSO_4$. At 300 s, the surface area and pore volume were decreased by 25.7% and 17.6%, respectively, for samples calcined with 0.3% SO_2.

Fig. 8 shows that when limestone particles were calcined in the presence of SO_2, the $CaSO_4$ formed changed the pore structure by filling or closing some pores. To determine how many pores were closed by the formed $CaSO_4$, a model based on the sulfation ratio and measured pore volume was established to calculate the closed-pore volume. Fig. 9 shows the schematic of a limestone particle calcined with or without SO_2. The calculation procedure is described as follows.

As in Fig. 9(a), the volume of the particle calcined without SO_2 consists of three elements, the volume of $CaCO_3$, CaO and open pores. When calcined in an atmosphere containing SO_2, the volume of the calcined particle consists of five elements, $CaCO_3$, CaO, $CaSO_4$, open pores and closed pores, as in Fig. 9(b). The basis of the calculation is that the pore volumes measured by the N_2 adsorption method do not include the volume of closed pores. An assumption made here is that SO_2 did not affect the sintering of the particle, and this assumption was also used in an investigation by Mahuli et al. [34].

Since the outer surface area of a calcined limestone particle contributes little to the full total surface area (assuming that the particle is a porous ball with porosity of 0.5, the inner surface area is about one hundred thousand times that of the outer surface), it is reasonable to assume that most of the $CaSO_4$ forms in the inner part of the particle. The volume of impurities was ignored based on the assumption that they did not react. On this basis, the full volume ($V_{A,0}$) of the particle calcined without SO_2 equals the full volume ($V_{A,1}$) of that calcined with SO_2.

$$V_{A,0} = V_{A,1} \tag{12}$$

(a) When limestone particles were calcined without SO_2:

$$V_{A,0} = V_{p,0} + V_{CaO,0} + V_{CaCO_3,0} \tag{13}$$

where $V_{p,0}$ is the open pore volume of the particle calcined without SO_2; $V_{CaO,0}$ and $V_{CaCO_3,0}$ are the volume of CaO and $CaCO_3$, respectively, as follows:

$$V_{p,0} = V_0 \cdot (M_{CaO} \cdot n \cdot X_{c,0} + M_{CaCO_3} \cdot n \cdot (1 - X_{c,0})) \tag{14}$$

$$V_{CaO,0} = V_{m,CaO} \cdot n \cdot X_{c,0} \tag{15}$$

$$V_{CaCO_3,0} = V_{m,CaCO_3} \cdot n \cdot (1 - X_{c,0}) \tag{16}$$

where V_0 is the measured specific pore volume; n is the total amount (in mol) of calcium in the particle; $V_{m,CaO}$ and $V_{m,CaCO_3}$ are the molar volume of CaO and $CaCO_3$, respectively; M_{CaO} and M_{CaCO_3} are the molar mass of CaO and $CaCO_3$, respectively; and $X_{c,0}$ is the calcination ratio.

(b) When limestone particles were calcined with SO_2:

$$V_{A,1} = V_{CaCO_{3,1}} + V_{CaO,1} + V_{CaSO_4,1} + V_{op,1} + V_{cp,1} \tag{17}$$

where $V_{CaCO_3,1}$, $V_{CaO,1}$, $V_{CaSO_4,1}$ are the volume of $CaCO_3$, CaO and $CaSO_4$,

respectively, in particles calcined with SO_2; and $V_{op,1}$ and $V_{cp,1}$ are the volume of open pores and closed pores, respectively.

The volume of $CaCO_3$, CaO, and $CaSO_4$ can be calculated by the calcination and sulfation ratios of the particle:

$$V_{\mathrm{CaCO_3},1} = V_{\mathrm{m,CaCO_3}} \cdot n \cdot (1 - X_{\mathrm{c}}) \tag{18}$$

$$V_{\mathrm{CaSO_4},1} = V_{\mathrm{m,CaSO_4}} \cdot n \cdot X_{\mathrm{s}} \tag{19}$$

$$V_{\mathrm{CaO},1} = V_{\mathrm{m,CaO}} \cdot n \cdot (X_{\mathrm{c},1} - X_{\mathrm{s}}) \tag{20}$$

where $V_{\mathrm{m,CaSO_4}}$ is the mole volume of $CaSO_4$; and X_{s} and $X_{\mathrm{c},1}$ are the sulfation ratio and calcination ratio of particles in the simultaneous calcination/sulfation reaction, respectively.

The volume of open pores is:

$$V_{\mathrm{op},1} = V_1 m_1 \tag{21}$$

where V_1 is the measured specific pore volume. The volume of closed pores is:

$$V_{\mathrm{cp},1} = V_{\mathrm{c},1} m_1 \tag{22}$$

where $V_{\mathrm{c},1}$ is the specific pore volume of closed pores.

The mass of the calcined particles m_1 is:

$$m_1 = n \cdot [(1 - X_{\mathrm{c},1}) M_{\mathrm{CaCO_3}} + (X_{\mathrm{c},1} - X_{\mathrm{s}}) \cdot M_{\mathrm{CaO}} + X_{\mathrm{s}} \cdot M_{\mathrm{CaSO_4}}] \tag{23}$$

Combining the formulas above, one can obtain:

$$V_{\mathrm{c},1} = \frac{k_1 V_0 + k_2 V_{\mathrm{m,CaO}} + k_3 V_{\mathrm{m,CaCO_3}} - X_{\mathrm{s}} V_{\mathrm{m,CaSO_4}}}{k_4 M_{\mathrm{CaCO_3}} + k_5 M_{\mathrm{CaO}} + X_{\mathrm{s}} M_{\mathrm{CaSO_4}}} - V_1 \tag{24}$$

in which

$$\begin{cases} k_1 = X_{c,0} M_{CaO} + (1 - X_{c,0}) M_{CaCO_3} \\ k_2 = X_{c,0} - (X_{c,1} - X_s) \\ k_3 = X_{c,1} - X_{c,0} \\ k_4 = 1 - X_{c,1} \\ k_5 = X_{c,1} - X_s \end{cases}$$

Formula (24) gives the closed-pore volume ($V_{c,1}$) of particles calcined in the presence of SO_2. The calculated results of closed-pore volumes at different times are shown in Fig. 10.

As shown in Fig. 10, the closed-pore volumes are larger than zero, which means that some pores are closed by the produced $CaSO_4$ as speculated. As the calcination proceeds, the closed-pore volume increases. At 300 s, the closed-pore volume is about 10% of the total pore volume. The increase of the closed-pore volume should be due to the accumulation of $CaSO_4$ in pores. As has been noted by Bhatia and Perlmutter [35], the closure of pores will occur when the solid product formed occupies a larger volume than the reactant consumed, and the pore closure will first occur at the surface, stopping further diffusion of the reactant gas.

It is also evident that some pores will be filled or even closed by the formed $CaSO_4$, so the pathways left for the diffusion of CO_2 will be lower, and the diffusion resistance should be increased. To further show the influence of $CaSO_4$ on the CO_2 diffusion resistance and the calcination rate quantitatively, the effectiveness factors for the calcination reaction with SO_2 were calculated and compared with those without SO_2.

The definition of the effectiveness factor η for a gas-solid reaction is [36]:

$$\eta = \frac{\text{actual reaction rate}}{\begin{array}{l}\text{reaction rate obtainable without}\\ \text{mass and heat diffusion resistance}\end{array}} \tag{25}$$

The effectiveness factor describes quantitatively to what degree the diffusion resistance slows down the reaction rate. For a spherical particle, η can be calculated by [36]:

$$\eta = \frac{3}{\phi}\left[\coth(\phi) - \frac{1}{\phi}\right] \tag{26}$$

$$\phi = R\sqrt{k_v / D_e} \tag{27}$$

where R is the radius of the particle, m; k_v is the reaction rate constant per unit volume; and D_e is the diffusion coefficient of CO_2 in pores of CaO layer. The procedure to calculate k_v and D_e can be found elsewhere [23]. The effectiveness factors at different times for calcination with 0.3% SO_2 are shown in Fig. 11, compared with those without SO_2.

Fig. 11 shows that the effectiveness factors η are all larger than 0.79 but lower than 0.85. According to Fogler [37], η in this range means that the calcination reaction was controlled by both the intrinsic reaction and the diffusion resistance in the pore, but the intrinsic reaction played a major role.

Under both conditions, the effectiveness factors for the calcination reaction decreased with time, which means that the diffusion resistance of CO_2 increased with the calcination process. For calcination without SO_2, the effectiveness factors decreased from 0.845 at 75 s to 0.822 at 300 s. With 0.3% SO_2, the effectiveness factors are about 2.5-3.6% lower than those without SO_2 for the entire calcination process. The $CaSO_4$ formed in the pores of the CaO layer should account for the

difference. Moreover, a lower effectiveness factor means that the diffusion resistance of CO_2 is higher for calcination in the presence of SO_2.

Combining data from Fig. 8, Fig. 10 and Fig. 11, the mechanism of the effect of SO_2 on calcination of limestone can be elucidated. When calcination of a limestone particle was proceeding, pores formed in the CaO layer served as the CO_2 diffusion path. On the other hand, in the presence of SO_2, $CaSO_4$ formed in the CaO layer, the pores were filled or even blocked by the formed $CaSO_4$, and pores remaining for the diffusion of CO_2 were less, resulting in an increase of the diffusion resistance of CO_2, consequently increasing the CO_2 partial pressure in the particle and decreasing the calcination rate.

Mechanism of the combined effect of H_2O and SO_2 on limestone calcination

As shown in Fig. 3, H_2O and SO_2 can change the calcination rate together, but H_2O played a more major role. This phenomenon must relate to both the intrinsic reaction rate and CO_2 diffusion resistance in the pores. To explain it, the pore structure of CaO under different conditions was measured first, then the CO_2 diffusion coefficients and effectiveness factors were calculated and analyzed.

Limestone particles experiencing the same calcination time (300 s) under different conditions (0 or 15% H_2O, 0 or 0.3% SO_2) were collected, and their surface area, pore volume, and pore size distribution were measured by the N_2 adsorption method, as shown in Fig. 12 and Fig. 13.

Considering the conditions without SO_2, as shown in Fig. 12, compared with conditions without H_2O, the surface area and pore volume of samples calcined in the

presence of 15% H_2O decreased by 34.2% and 51.7%, respectively. In Fig. 13, both peaks of the pore size distribution were decreased by H_2O. These phenomena illustrate that H_2O causes a significant enhancement of the sintering of CaO.

Fig. 12 shows that the pore volume and surface area under 15% H_2O and 0.3% SO_2 were the lowest. This indicates that the filling effect of SO_2 and the enhanced sintering effect of H_2O can act synergistically in decreasing the pore volume and surface area. This synergy effect can also be found from Fig. 13, in which the pore size distribution of CaO generated in 15% H_2O and 0.3% SO_2 has the lowest peak value.

To analyze the effect of pore structure on reaction rate, the effective diffusion coefficients D_e and effectiveness factors η for the calcination under different conditions were calculated based on the pore parameters in Fig. 12. The results are shown in Table 5.

From Table 5, it can be seen that both D_e and η under 15% H_2O were lower than those without H_2O. The enhanced sintering of CaO by H_2O, which decreased the pore volume, should be the main cause for the lower D_e. At the same time, the lower D_e and higher intrinsic calcination rate result in the lower η. Although the effectiveness factors under 15% H_2O were lower, the calcination rate was higher, as shown Fig. 3. This means that the intrinsic reaction rather than CO_2 diffusion resistance played the major role in the rate-controlling step.

As discussed in Fig. 3, the calcination rate of particles with both 15% H_2O and 0.3% SO_2 was larger than that without them, but lower than that with only 15% H_2O

and no SO_2. This can be explained by the findings presented in Fig. 7 and Table 5, that the intrinsic reaction played a major role in the controlling step of the calcination reaction. Since H_2O can increase the intrinsic reaction by catalysis, the influence of 15% H_2O was clearly stronger than 0.3% SO_2 concentration in changing the reaction rate, and in consequence, calcination rate under 15% H_2O and 0.3% SO_2 was larger than that without these two components.

Sulfur capture optimization in CFB boiler

Sulfur capture based on simultaneous calcination/sulfation reaction

In Fig. 2, it was found that the sulfation ratio of limestone experiencing the simultaneous calcination/sulfation reaction is different from that occurring via the calcination-then-sulfation reaction. Therefore, assuming the latter to analyze the sulfur capture performance of limestone, as is implicitly done [38], will produce errors. To demonstrate this further, the limestone consumption in a 600 MWe CFB burning petroleum coke was calculated. For comparison, the calculation was based on the calcium utilization data from the simultaneous calcination/sulfation reaction and calcination-then-sulfation reaction, respectively, and the data were obtained from the system in Fig. 1.

Table 6 shows the analysis of the petroleum coke (as received basis) [39] used for these calculations. As is typical of petroleum coke, its sulfur content is high but ash content is very low, so the self-desulfurization efficiency can be ignored. When burning the petroleum coke, the SO_2 concentration in flue gas is about 0.3% (with excess air coefficient of 1.4) and (assuming) the standard fuel consumption rate for

power generation is 0.3 kg/kWh.

The calcium utilization and limestone consumption needed to reach a desulfurization efficiency of 90% under different reaction modes are compared in Fig. 14. The sulfation ratios of limestone and CaO (0.4-0.45 mm Baoding, sulfated for 90 min at 850 °C and 0.3% SO_2) were taken as the calcium utilization for the calculation.

As shown in Fig. 14, compared with that in the calcination-then-sulfation reaction, the calcium utilizations in the simultaneous calcination/sulfation reaction were much higher, while the limestone consumptions to reach the same desulfurization efficiency were much lower. Taking condition of 8% H_2O for example, the difference in calcium utilization or limestone consumption was about 25%.

Thus, when evaluating the sulfur capture performance of limestone, the data from the sulfation of CaO can produce major errors. Therefore, the simultaneous calcination/sulfation reaction, rather than the sulfation of CaO, should be adopted in future to evaluate the sulfation performance of limestone.

Based on the calcium utilization data from the simultaneous calcination/sulfation reaction, the influence of H_2O and SO_2 concentration on the sulfur capture characteristics in a CFB can be accurately analyzed further. The desulfurization efficiency and SO_2 emission at Ca/S=3, and the limestone consumption to reach a desulfurization efficiency of 90% in the CFB under different H_2O and SO_2 concentration are calculated and shown in Fig. 15.

Fig. 15(a) shows that the calcium utilization increases with H_2O concentration in the range of 0-25%. The research of Jiang et al. [19] found that the sulfation ratio of

CaO can still increase with H_2O even at levels as high as 40%, albeit that this would produce other problems. At the same time, the limestone consumption rate to reach a desulfurization efficiency of 90% decreases significantly. A higher calcium utilization can improve the desulfurization efficiency in a CFB, and consequently, SO_2 emission declines sharply, as shown in Fig. 15(b). Assuming conditions of 0.3% SO_2, for example, when H_2O concentration increases from 0 to 25%, the SO_2 emission at *Ca/S*=3 decreases from 5.84 t/h to 1.1 t/h.

Fig. 15 shows that the SO_2 concentration can also influence the sulfur capture characteristics. With a higher concentration of SO_2, the calcium utilization also increases, which can improve the desulfurization efficiency and lead to a lower SO_2 emission. Taking conditions of 8% H_2O as our example, when SO_2 concentration increases from 0.15% to 0.3%, the SO_2 emissions fall from 7.34 t/h to 3.94 t/h. Under different SO_2 concentration, the effect of H_2O on SO_2 capture was almost the same.

It is worth noting that the comparison in Fig. 14 and Fig. 15 focused only on the effect of water vapor and SO_2 content on sulfur capture in CFB boilers, but many other factors also play an important role, such as limestone size and quality, cyclone efficiency, oxygen supply to the furnace (oxidizing and reducing conditions), etc. [1, 4] These factors can affect the sulfur capture performance significantly, and although outside the scope of this work, should also be investigated.

Optimizing the sulfur capture in CFBs

One of the main problems of the in-situ desulfurization in CFBs is the low calcium utilization. Investigators have recommended many ways to improve the calcium

utilization, for example, operating temperature optimization [40] and limestone particle size optimization [41].

Based on the findings of Fig. 15, another method can be proposed to optimize the sulfur capture in CFBs, the wet flue gas recycle. Namely, when burning coals containing high sulfur but low moisture, increasing H_2O concentration could increase the calcium utilization and desulfurization efficiency according to Fig. 15.

Duan et al. [42] reported that the desulfurization efficiency in oxy-fuel CFB can be increased by wet flue gas recycle, due to the high steam concentration. It is clear from this work, in air-fired CFBs, wet flue gas recycle can also increase the H_2O partial pressure in the furnace, and ought to improve the desulfurization performance as well. While these findings are preliminary and will require significantly more work to extend them to various coal types, or coal firing modes such as co-firing, it is evident that they are potentially very significant.

Conclusions

The combined effect of H_2O and SO_2 on the reaction kinetics and pore structure of limestone during simultaneous calcination/sulfation reactions under CFB conditions was studied in a constant-temperature reactor. The following conclusions were drawn:

(1) H_2O can accelerate the sulfation rate in the slow-sulfation stage significantly, but has less effect on the fast-sulfation stage. H_2O can catalyze the calcination of $CaCO_3$, and this is supported by the lower calcination activation energy observed in the presence of H_2O.

(2) SO_2 in the flue gas decreased the calcination rate of limestone particles. SO_2 reacts with the CaO layer, and the formed $CaSO_4$ fills or blocks the pores in CaO layer, decreases the pore volume, increases the diffusion resistance of CO_2, and consequently impedes the calcination reaction.

(3) The acceleration by H_2O and the deceleration by SO_2 on the calcination reaction rate can occur together. Intrinsic reaction played a major role in the calcination rate-controlling step, and an increase in the calcination rate was found under 15% H_2O and 0.3% SO_2 as compared to that observed without either.

(4) The sulfation performance of limestone evaluated by simultaneous calcination/sulfation is much higher than that by sulfation of CaO. Hence, the simultaneous calcination/sulfation reaction, rather than the sulfation of CaO, should be adopted when evaluating the SO_2 capture performance of limestone.

(5) Some degree of wet flue gas recycle should help to optimize the sulfur capture in CFBs when burning low-moisture fuels, because higher H_2O and SO_2 concentrations can increase the calcium sulfation degree.

Acknowledgement

This work was supported by the National Key R&D Program of China [2016YFB0600701]; and the Fundamental Research Funds for the Central Universities [2018ZD03].

References

1. Anthony EJ, Granatstein DL. Sulfation phenomena in fluidized bed combustion systems. *Prog Energ Combust*. 2001;27(2):215-236.
2. Wu Y, Wang C, Tan Y, Jia L, Anthony EJ. Characterization of ashes from a 100kWth pilot-scale circulating fluidized bed with oxy-fuel combustion. *Appl Energ*. 2011;88(9):2940-2948.
3. Tan Y, Jia L, Wu Y, Anthony EJ. Experiences and results on a 0.8MWth oxy-fuel operation pilot-scale circulating fluidized bed. *Appl Energ*. 2012;92:343-347.
4. Altindag H, Gogebakan Y, Selçuk N. Sulfur capture for fluidized-bed combustion of high-sulfur content lignites. *Appl Energ*. 2004;79(4):403-424.
5. Borgwardt RH. Calcination Kinetics and Surface Area of Dispersed Limestone Particles. *AIChE J*. 1985;31(1):103-111.
6. Gallagher PK, Johnson Jr DW. The effects of sample size and heating rate on the kinetics of the thermal decomposition of $CaCO_3$. *Thermochim Acta*. 1976;6(1):67-83.
7. Khinast J, Krammer GF, Brunner C, Staudinger G. Decomposition of limestone: The influence of CO_2 and particle size on the reaction rate. *Chem Eng Sci*. 1996;51(4):623-634.
8. Adánez J, Labiano FG, Abánades JC, Diego LFD. Methods for characterization used in fluidized bed boilers of sorbents. *Fuel*. 1994;73(1):355-362.
9. Borgwardt RH. Kinetics of the Reaction of SO_2 with Calcined Limestone. *Environ Sci Technol*. 1970;4(1):59-63.
10. Simons GA, Garman AR, Boni AA. The Kinetic Rate of SO_2 Sorption by CaO. *AIChE J*. 1987;33(2):211-217.
11. Wang C, Zhang Y, Jia L, Tan Y. Effect of water vapor on the pore structure and sulfation of CaO. *Fuel*. 2014;130:60-65.

12. Borgwardt RH, Bruce KR. Effect of Specific Surface Area on the Reactivity of CaO with SO_2. *AIChE J*. 1986;32(2):239-246.

13. Borgwardt RH. Calcium Oxide Sintering in Atmospheres Containing Water and Carbon Dioxide. *Ind Eng Chem Res*. 1989;28(4):493-500.

14. Wang Y, Thomson WJ. The effects of steam and carbon dioxide on calcite decomposition using dynamic X-ray diffraction. *Chem Eng Sci*. 1995;50(9):1373-1382.

15. Wang Y, Lin S, Suzuki Y. Limestone Calcination with CO_2 Capture (II) - Decomposition in CO_2-Steam and CO_2-N_2 Atmospheres. *Energ Fuel*. 2008;22(4):2326-2331.

16. Burnham AK, Stubblefield CT, Campbell JH. Effects of gas environment on mineral reactions in Colorado oil shale. *Fuel*. 1980;59(12):871-877.

17. Stewart MC, Manovic V, Anthony EJ, Macchi A. Enhancement of Indirect Sulphation of Limestone by Steam Addition. *Environ Sci Technol*. 2010;44(22):8781-8786.

18. Stewart MC, Symonds RT, Manovic V, Macchi A, Anthony EJ. Effects of steam on the sulfation of limestone and NOx formation in an air- and oxy-fired pilot-scale circulating fluidized bed combustor. *Fuel*. 2012;92(1):107-115.

19. Jiang Z, Duan L, Chen X, Zhao C. Effect of Water Vapor on Indirect Sulfation during Oxy-fuel Combustion. *Energ Fuel*. 2013;27(3):1506-1512.

20. Duan L, Jiang Z, Chen X, Zhao C. Investigation on water vapor effect on direct sulfation during wet-recycle oxy-coal combustion. *Appl Energ*. 2013;108(8):121-127.

21. Wang C, Chen L, Jia L, Tan Y. Simultaneous calcination and sulfation of limestone in CFBB. *Appl Energ*. 2015;155:478-484.

22. Wang C, Chen L. The effect of steam on simultaneous calcination and sulfation of limestone in

CFBB. *Fuel*. 2016;175:164-171.

23. Chen L, Wang C, Wang Z, Anthony EJ. The kinetics and pore structure of sorbents during the simultaneous calcination/sulfation of limestone in CFB. *Fuel*. 2017;208:203-213.

24. Hu G, Dam-Johansen K, Wedel S, Peterhansen J. Review of the direct sulfation reaction of limestone. *Prog Energ Combust*. 2006;32(4):386-407.

25. Manovic V, Anthony EJ. Parametric Study on the CO_2 Capture Capacity of CaO-Based Sorbents in Looping Cycles. *Energ Fuel*. 2008;22(3):1851-1857.

26. Lisbona P, Martínez A, Romeo LM. Hydrodynamical model and experimental results of a calcium looping cycle for CO_2 capture. *Appl Energ*. 2013;101:317-322.

27. Fan Y, Yao JG, Zhang Z, Sceats M, Zhuo Y, Li L, Maitland GC, Fennell PS. Pressurized calcium looping in the presence of steam in a spout-fluidized-bed reactor with DFT analysis. *Fuel Process Technol*. 2018;169:24-41.

28. Wang C, Zhou X, Jia L, Tan Y. Sintering of Limestone in Calcination/Carbonation Cycles. *Ind Eng Chem Res*. 2014;53(42):16235-16244.

29. Wang H, Guo S, Liu D, Guo Y, Gao D, Sun S. A Dynamic Study on the Impacts of Water Vapor and Impurities on Limestone Calcination and CaO Sulfurization Processes in a Microfluidized Bed Reactor Analyzer. *Energ Fuel*. 2016;30(6):4625-4634.

30. Baker EH. The Calcium Oxide-Carbon Dioxide System in the Pressure Range 1-300 Atmospheres. *Journal of the Chemical Society*. 1962;70:464-470.

31. Li Z, Liu Y, Cai N. Understanding the enhancement effect of high-temperature steam on the carbonation reaction of CaO with CO_2. *Fuel*. 2014;127:88-93.

32. Manovic V, Anthony EJ. Carbonation of CaO-Based Sorbents Enhanced by Steam Addition. *Ind*

Eng Chem Res. 2010;49(19):9105-9110.

33. Wang C, Jia L, Tan Y, Anthony EJ. Carbonation of fly ash in oxy-fuel CFB combustion. *Fuel*. 2008;87(7):1108-1114.

34. Mahuli SK, Agnihotri R, Chauk S, Ghosh-Dastidar A, Wei S, Fan L. Pore-structure optimization of calcium carbonate for enhanced sulfation. *AIChE J*. 1997;43(9):2323-2335.

35. Bhatia SK, Perlmutter DD. A Random Pore Model for Fluid-Solid Reactions: II. Diffusion and Transport Effects. *AIChE J*. 1981;27(2):247-254.

36. Ishida M, Wen CY. Comparison of Kinetic and Diffusional Models for Solid-Gas Reactions. *AIChE J*. 1968;14(2):311-317.

37. Fogler HS. Elements of Chemical Reaction Engineering (4th edition). New York: Prentice Hall PTR, 2006.

38. Shih S, Lai J, Yang C. Kinetics of the Reaction of Dense CaO Particles with SO_2. *Ind Eng Chem Res*. 2011;50(22):12409-12420.

39. Anthony EJ, Iribarne AP, Iribarne JV, Talbot R, Jia L, Granatstein DL. Fouling in a 160 MWe FBC boiler Firing Coal and Petroleum Coke. *Fuel*. 2001;80:1009-1014.

40. de Diego LF, de Las Obras-Loscertales M, Rufas A, García-Labiano F, Gayán P, Abad A, Adánez J. Pollutant emissions in a bubbling fluidized bed combustor working in oxy-fuel operating conditions: Effect of flue gas recirculation. *Appl Energ*. 2013;102:860-867.

41. Saastamoinen JJ, Shimizu T, Tourunen A. Effect of attrition on particle size distribution and SO_2 capture in fluidized bed combustion under high CO_2 partial pressure conditions. *Chem Eng Sci*. 2010;65(1):550-555.

42. Duan L, Sun H, Zhao C, Zhou W, Chen X. Coal combustion characteristics on an oxy-fuel

circulating fluidized bed combustor with warm flue gas recycle. *Fuel*. 2014;127:47-51.

Table 1. Limestone Composition.

Compound (%)	SiO_2	Al_2O_3	Fe_2O_3	TiO_2	P_2O_5	CaO	MgO	SO_3	Na_2O	K_2O	Loss on Fusion
Baoding	0.67	0.78	<0.10	<0.05	<0.03	54.93	<0.10	<0.10	<0.10	<0.10	42.90
Xinxiang	0.45	0.56	0.15	0.05	<0.03	55.02	0.48	<0.10	<0.20	0.24	42.78

Table 2. Pore structures of the two limestones

parameters	Baoding limestone	Xinxiang limestone
pore surface area, S (m^2/g)	23.7	17.1
pore volume, V (cm^3/g)	0.261	0.225
average pore width, $4V/S$ (nm)	44.0	52.6

Table 3. Experimental conditions.

Conditions	Value
Temperature (°C)	820, 850, 880, 910
CO_2 concentration (%)	15
O_2 concentration (%)	3
SO_2 concentration (%)	0, 0.15, 0.3
H_2O concentration (%)	0, 8, 15, 25
N_2 concentration (%)	Balance
Particle size (mm)	0.4-0.45

Table 4. Kinetic parameters for limestone calcination.

Conditions	Correlation equation	E_a (kJ/mol)	k_0 (s^{-1})	Correlation coefficient (-)
0% H_2O	$\ln(k_c)$=21.4-17848/T	148.4	1.97×10^9	0.99
15% H_2O	$\ln(k_c)$=19.5-15583/T	129.6	0.30×10^9	0.99

Table 5. The effective diffusion coefficients and effectiveness factors.

H_2O (%)	SO_2 (%)	D_e (10^{-6} cm^2/s)	η (-)
0	0	24878	0.823
0	0.3	20532	0.796
15	0	16423	0.728
15	0.3	12067	0.671

Table 6. Analysis of a petroleum coke (mass fraction, %).

component	value	component	value
M_{ar}	0.63	H_{ar}	3.42
A_{ar}	0.48	O_{ar}	1.58
V_{ar}	10.17	N_{ar}	1.48
FC_{ar}	88.72	S_{ar}	5.57
C_{ar}	86.84	Q_{ar}	34.2 (MJ/kg)

Figure Captions

Fig. 1. The experimental system.

Fig. 2. Effect of H_2O on simultaneous calcination/sulfation reaction

Fig. 3. Effect of 15% H_2O and 0.3% SO_2 on calcination of limestone. (a) The change of sample mass; (b) the percent calcination ratio of samples.

Fig. 4. Effect of H_2O on calcination of limestone with 0.3% SO_2. (a) The change of sample mass; (b) the percent calcination ratio of samples.

Fig. 5. Effect of SO_2 on calcination of limestone with 15% H_2O. (a) The change of sample mass; (b) the percent calcination ratio of samples.

Fig. 6. Combined effect of H_2O and SO_2 on Xinxiang limestone. (a) The change of sample mass; (b) the percent calcination ratio of samples.

Fig. 7. Influence of H_2O on kinetic parameters for limestone calcination.

Fig. 8. Pore structure of particles in calcination process. (a) Surface area; (b) pore volume.

Fig. 9. Schematic of a particle. (a) Calcined without SO_2; (b) calcined with SO_2.

Fig. 10. The closed-pore volume of limestone particles calcined in 0.3% SO_2.

Fig. 11. Effect of SO_2 on the effectiveness factors of the calcination reaction.

Fig. 12. Influence of H_2O and SO_2 on pore structure. (a) Surface area; (b) pore volume.

Fig. 13. Influence of H_2O and SO_2 on the pore size distribution.

Fig. 14. The calcium utilization and limestone consumption to reach a desulfurization efficiency of 90% based on simultaneous calcination/sulfation mode compared with that based on calcination-then-sulfation mode.

Fig. 15. Effect of H_2O and SO_2 concentration on sulfur capture characteristics in 600 MWe CFB burning petroleum coke. (a) calcium utilization, and limestone consumption to reach a desulfurization efficiency of 90%; (b) desulfurization efficiency and SO_2 emission at *Ca/S*=3.

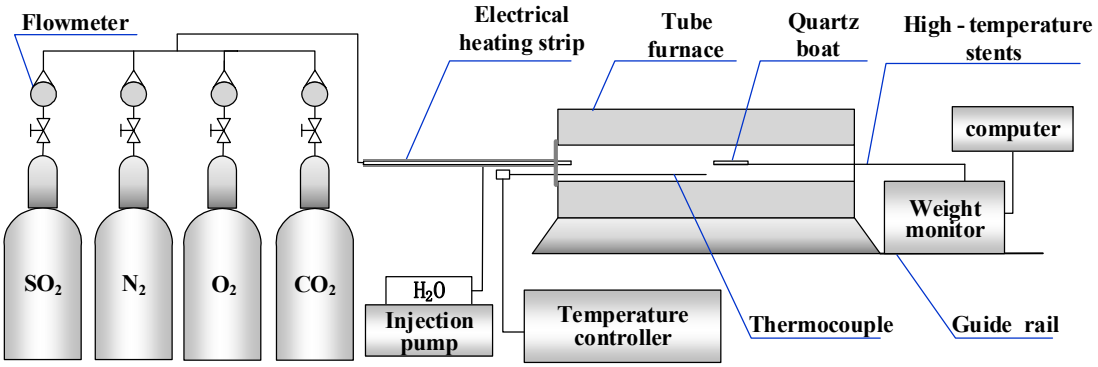

Fig. 1. The experimental system.

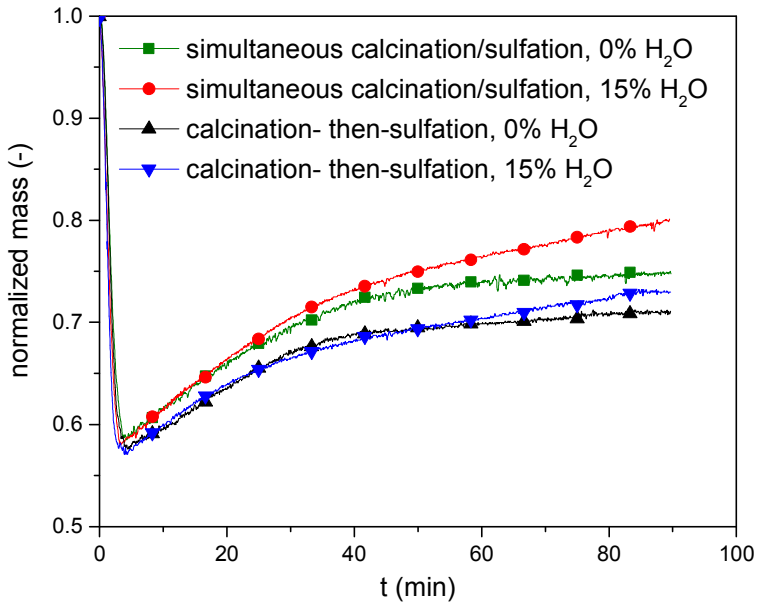

Fig. 2. Effect of H_2O on simultaneous calcination/sulfation reaction

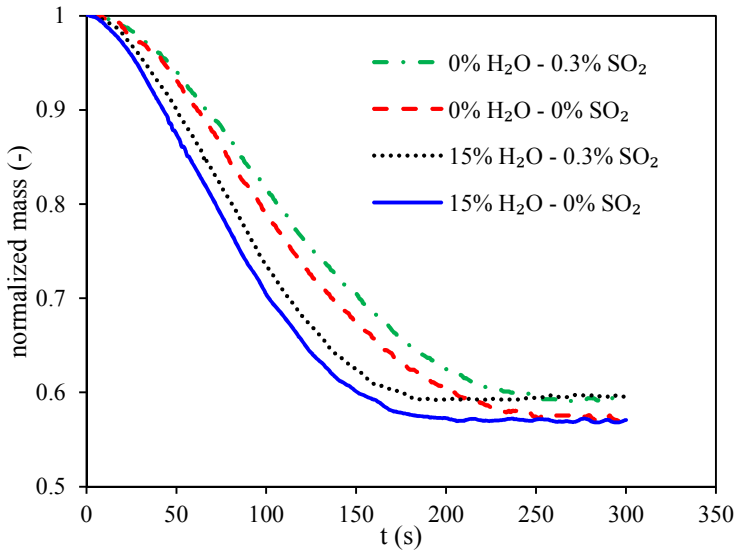

(a)

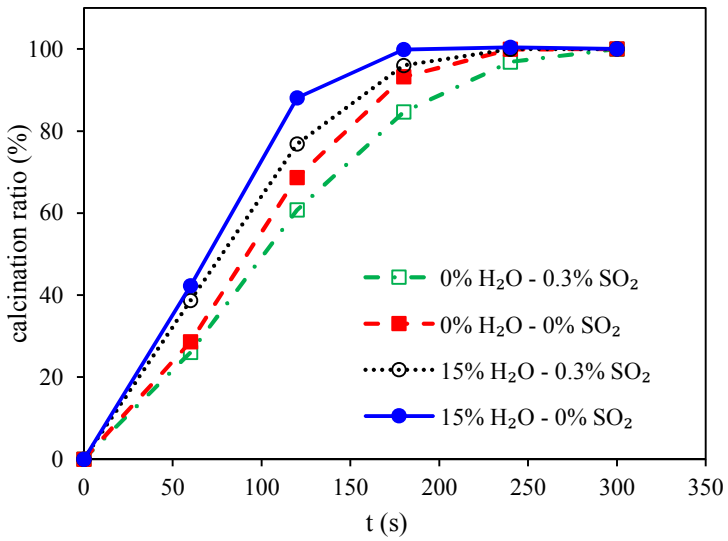

(b)

Fig. 3. Effect of 15% H_2O and 0.3% SO_2 on calcination of limestone. (a) The change of sample mass; (b) the percent calcination ratio of samples.

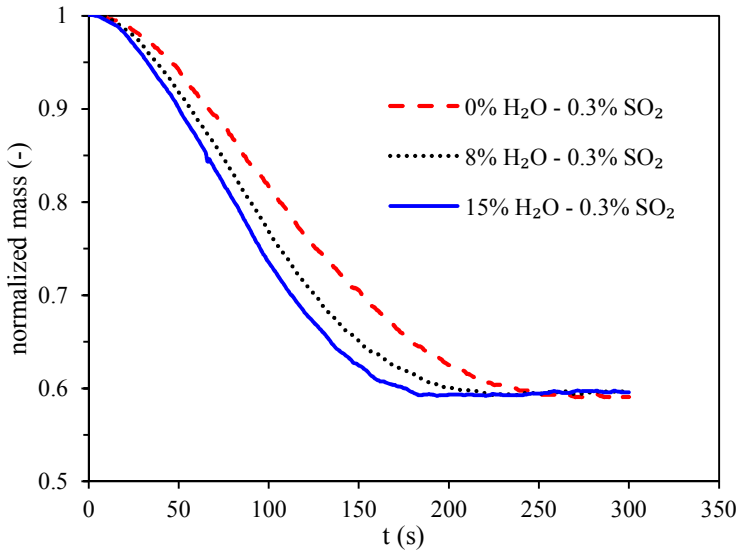

(a)

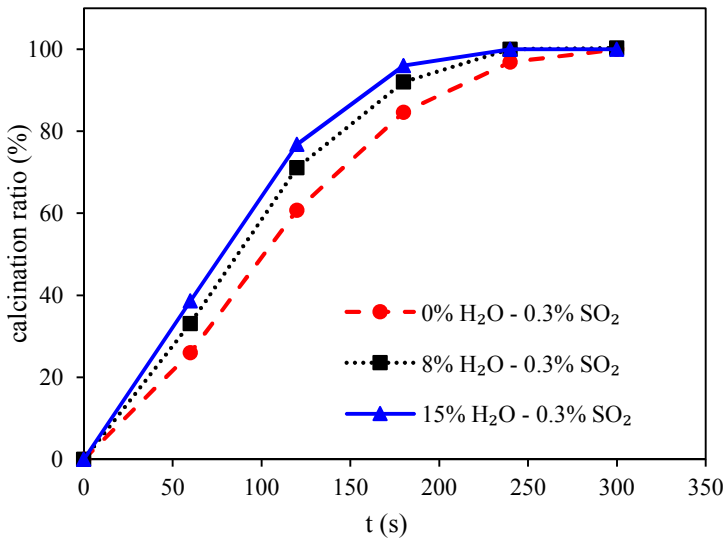

(b)

Fig. 4. Effect of H_2O on calcination of limestone with 0.3% SO_2. (a) The change of sample mass; (b) the percent calcination ratio of samples.

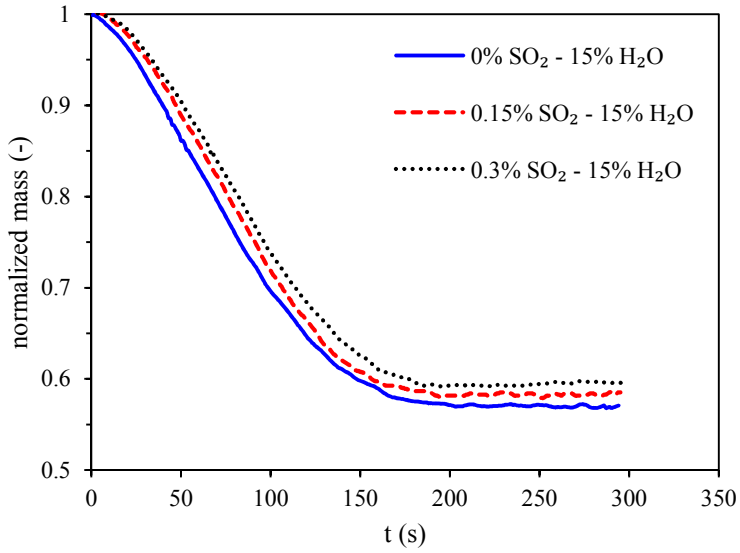

(a)

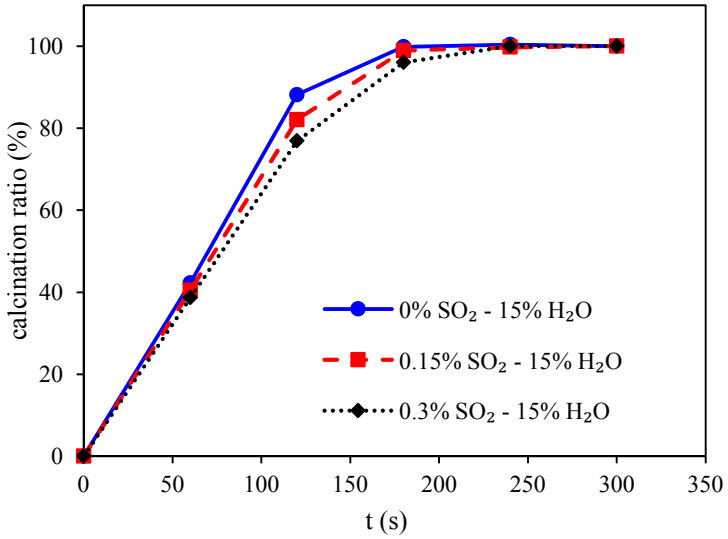

(b)

Fig. 5. Effect of SO_2 on calcination of limestone with 15% H_2O. (a) The change of sample mass; (b) the percent calcination ratio of samples.

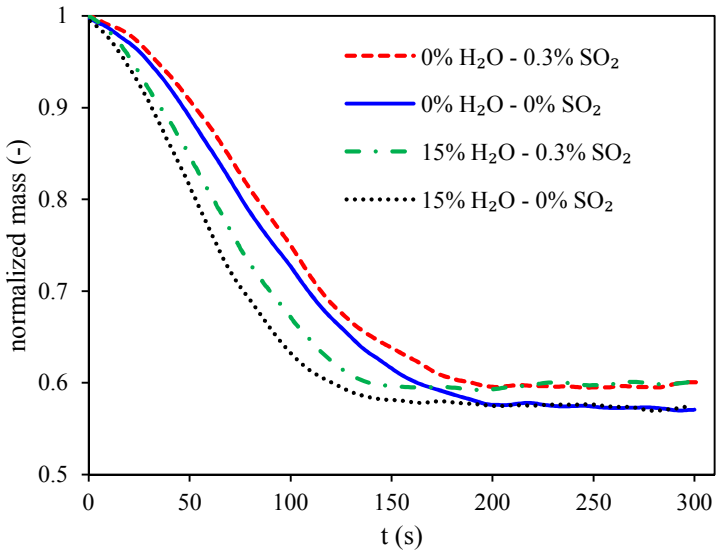

(a)

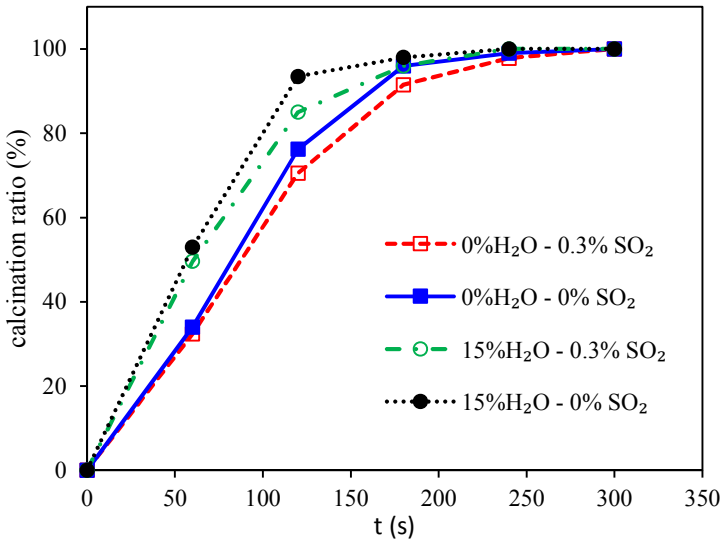

(b)

Fig. 6. Combined effect of H_2O and SO_2 on Xinxiang limestone. (a) The change of sample mass; (b) the percent calcination ratio of samples.

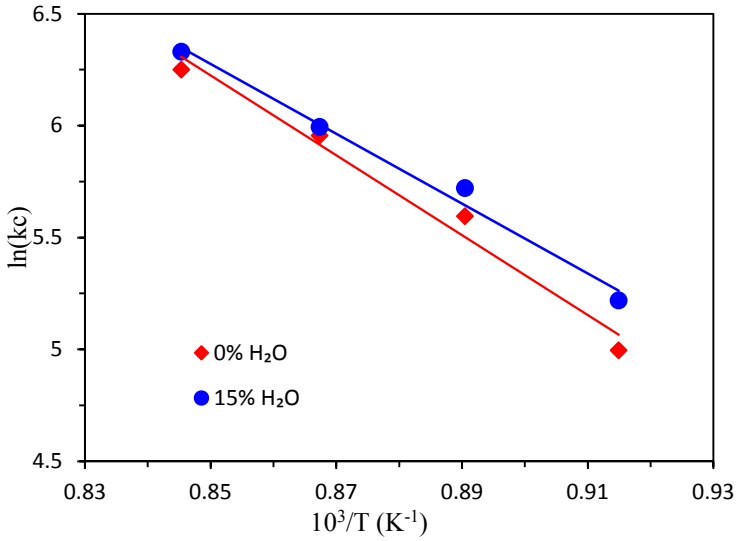

Fig. 7. Influence of H_2O on kinetic parameters for limestone calcination.

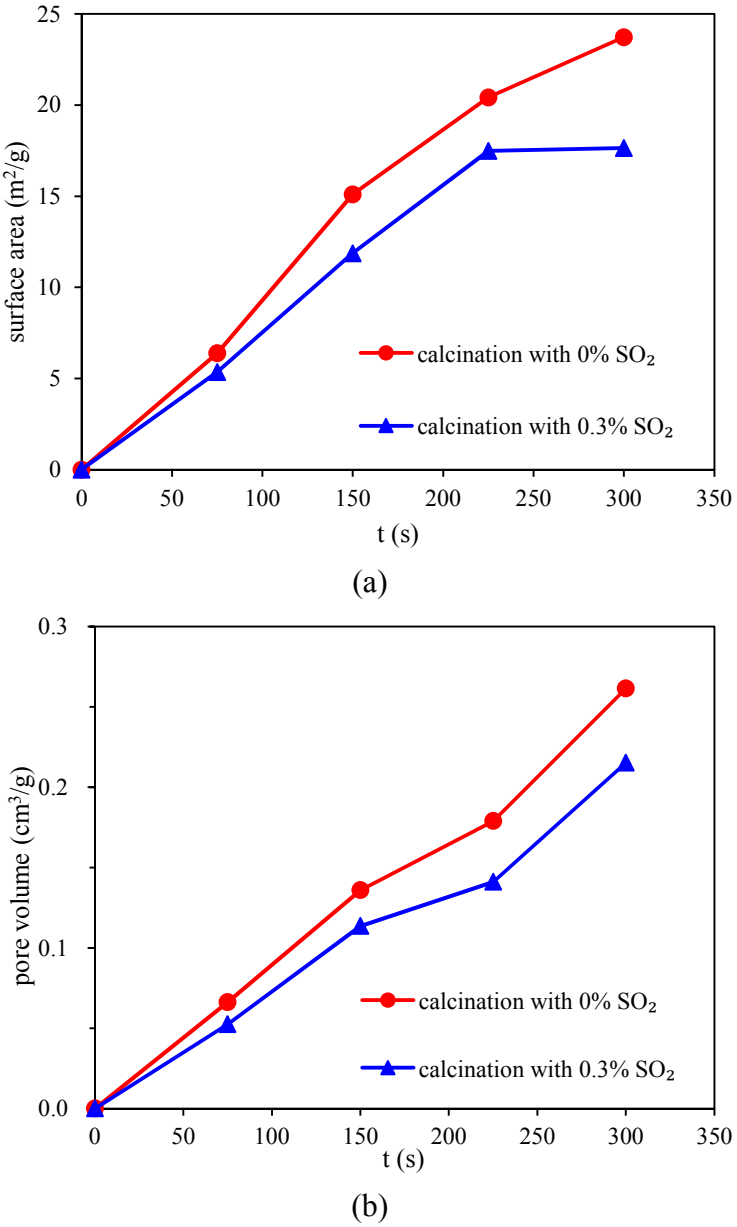

Fig. 8. Pore structure of particles in calcination process. (a) Surface area; (b) pore volume.

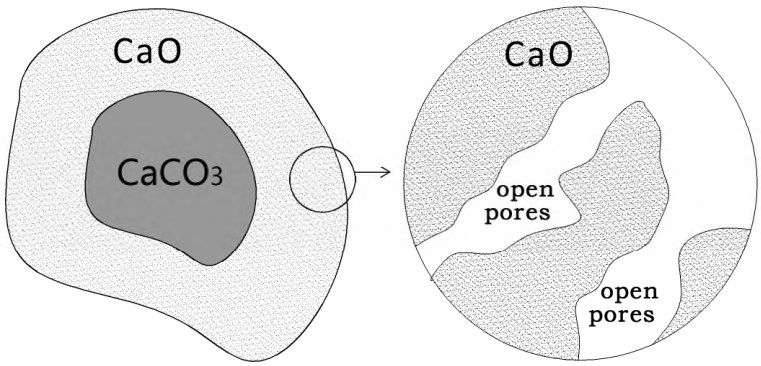

(a)

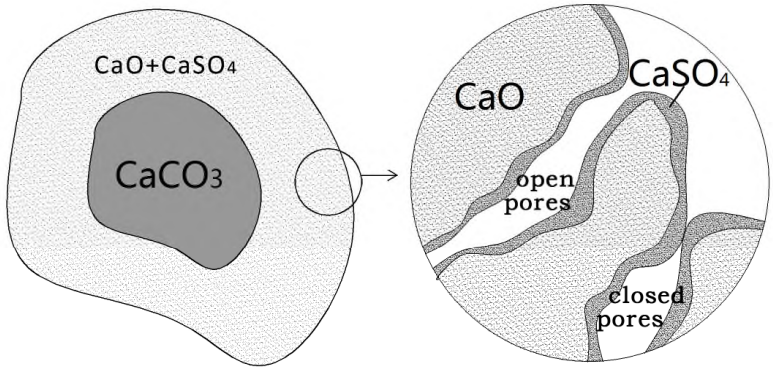

(b)

Fig. 9. Schematic of a particle. (a) Calcined without SO_2; (b) calcined with SO_2.

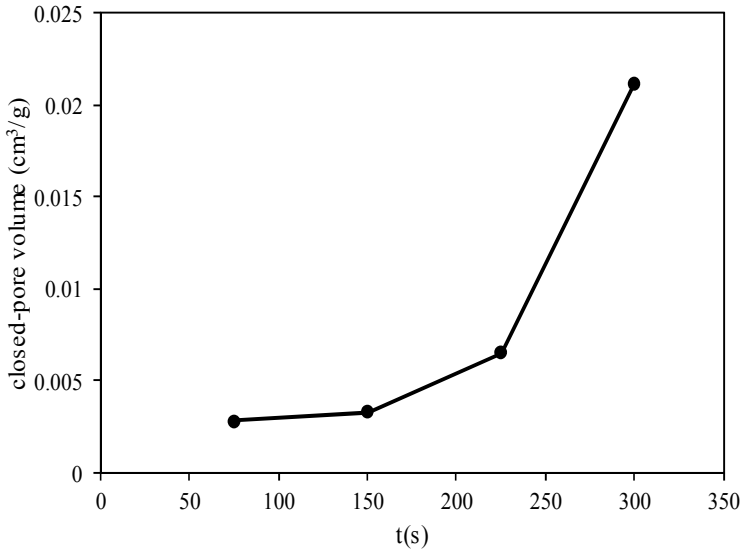

Fig. 10. The closed-pore volume of limestone particles calcined in 0.3% SO_2.

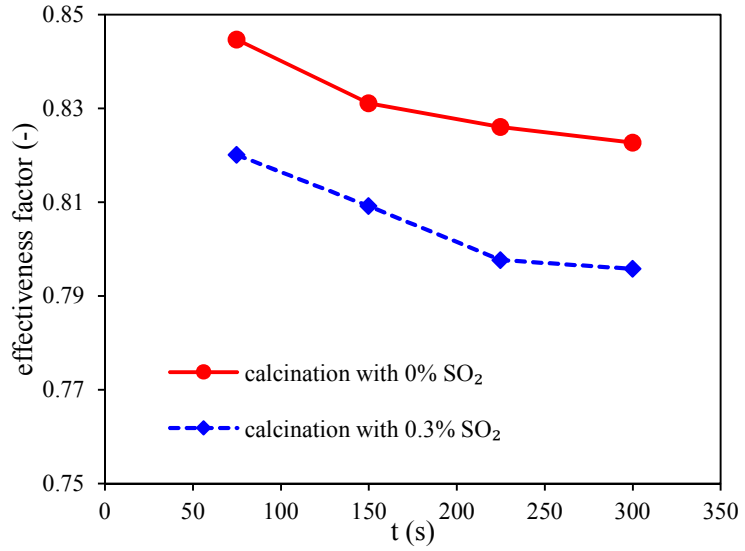

Fig. 11. Effect of SO_2 on the effectiveness factors of the calcination reaction.

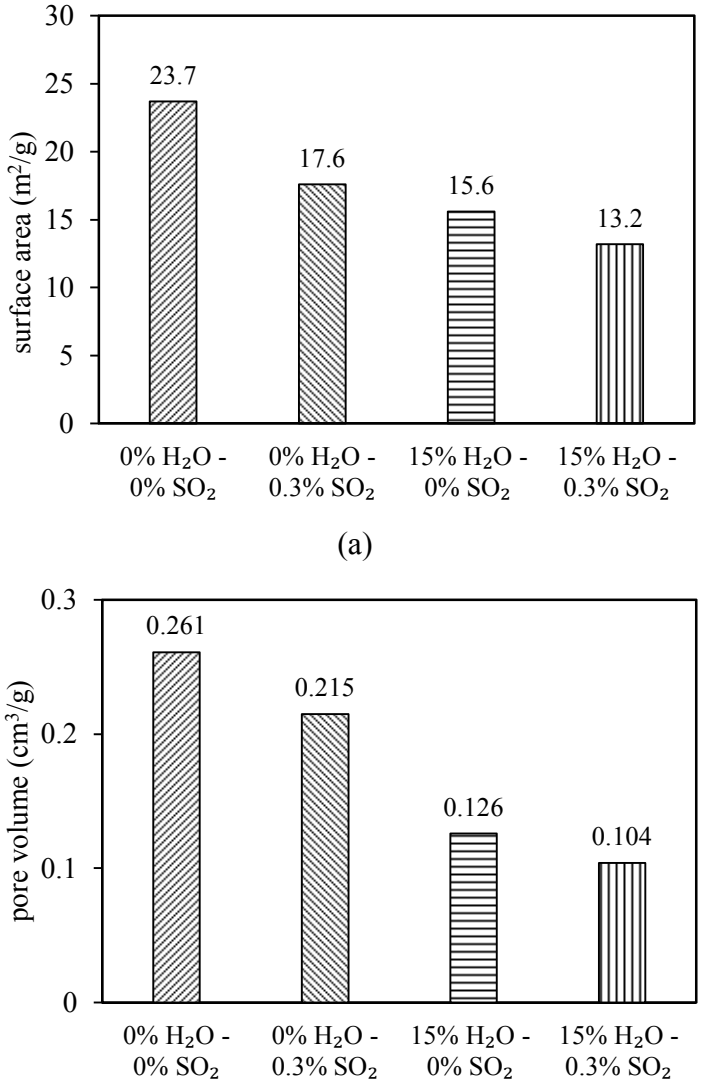

Fig. 12. Influence of H_2O and SO_2 on pore structure. (a) Surface area; (b) pore volume.

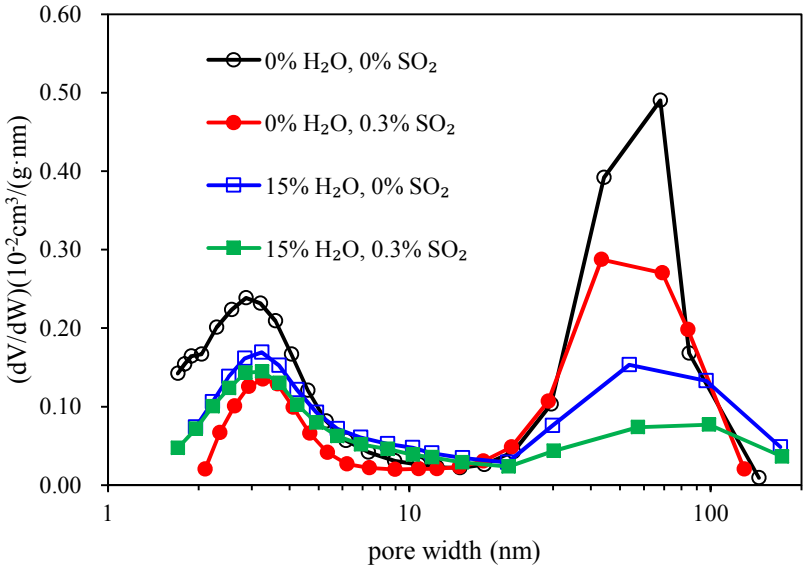

Fig. 13. Influence of H_2O and SO_2 on the pore size distribution.

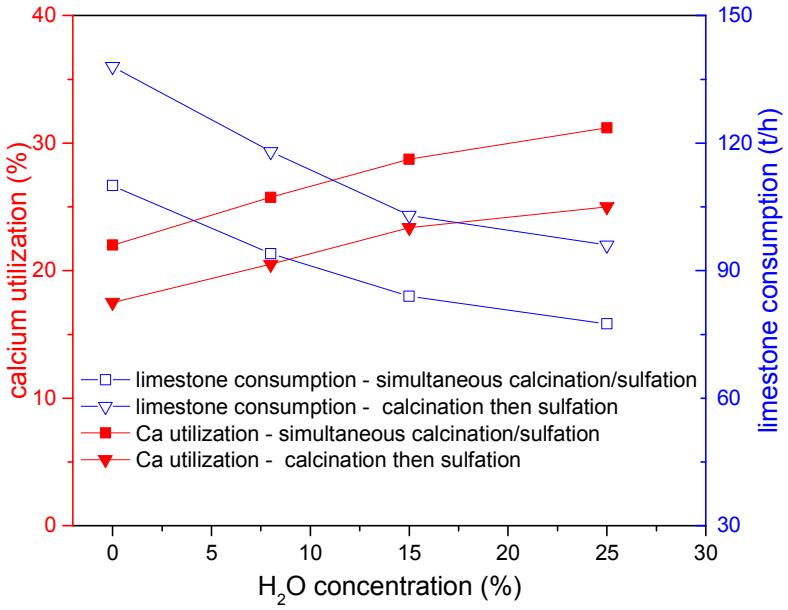

Fig. 14. The calcium utilization and limestone consumption to reach a desulfurization efficiency of 90% based on simultaneous calcination/sulfation mode compared with that based on calcination-then-sulfation mode.

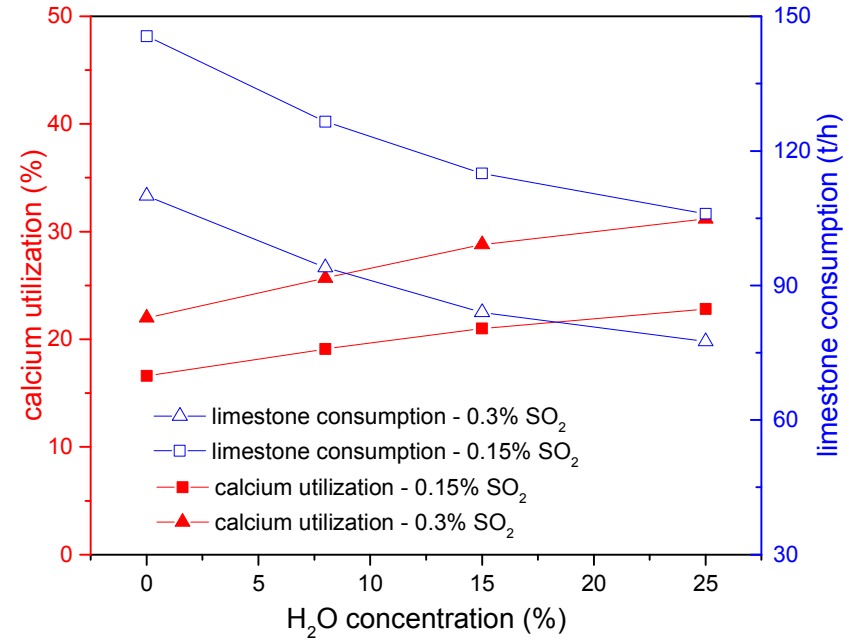

(a)

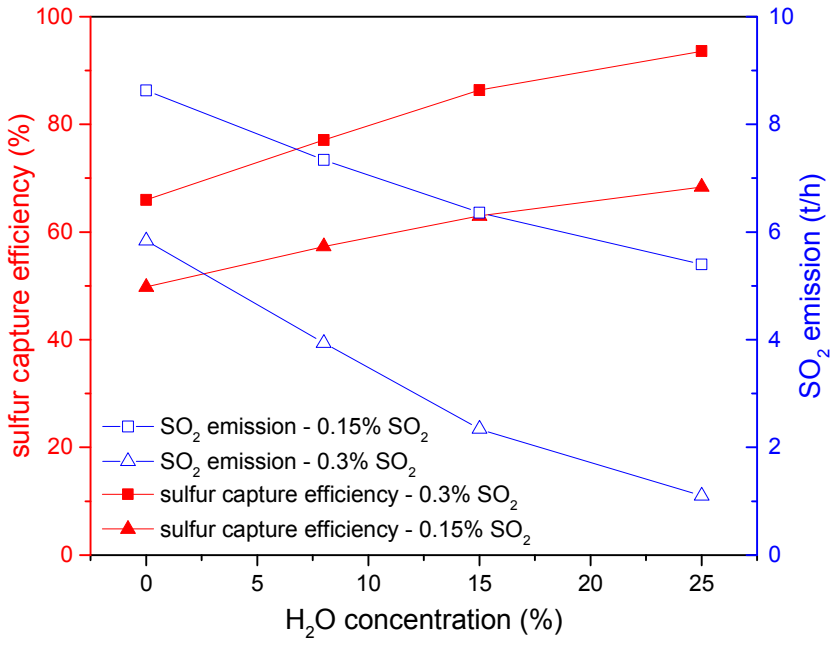

(b)

Fig. 15. Effect of H_2O and SO_2 concentration on sulfur capture characteristics in 600 MWe CFB burning petroleum coke. (a) calcium utilization, and limestone consumption to reach a desulfurization efficiency of 90%; (b) desulfurization efficiency and SO_2 emission at *Ca/S*=3.

https://dspace.org/

The combined effect of H2O and SO2 on the simultaneous calcination/sulfation reaction in CFBs

Chen, Liang; Wang, Chunbo; Zhao, Fan; Zou, Chan; Anthony, Edward J.

2019-01-10
Wiley
https://doi.org/10.1002/aic.16531
Chen L, Wang C, Zhao F, et al., The combined effect of H2O and SO2 on the simultaneous calcination/sulfation reaction in CFBs. AIChE Journal, Volume 65, Issue 4, April 2019, pp. 1256-1268

Downloaded from a DSpace repository. https://dspace.org/